



# Green synthesis of zinc oxide catalyst under microwave irradiation using banana (*Musa spp.*) corm (rhizome) extract for biodiesel synthesis from fish waste lipid

Swapnamoy Dutta<sup>a,1</sup>, Krishna Kumar Jaiswal<sup>a,b,1</sup>, Ravikant Verma<sup>c</sup>,  
Divakara Madhihalli Basavaraju<sup>d</sup>, Arun Prasath Ramaswamy<sup>a,\*</sup>

<sup>a</sup> Laboratory for Energy Materials and Sustainability, Centre for Green Energy Technology, Pondicherry University, Puducherry, 605014, India

<sup>b</sup> Algae Research & Bio-energy Laboratory, Department of Chemistry, Uttarakhand University, Dehradun, Uttarakhand, 248007, India

<sup>c</sup> Department of Ecology and Environmental Sciences, Pondicherry University, Puducherry, 605014, India

<sup>d</sup> Center for Incubation, Innovation, Research and Consultancy, Jyothy Institute of Technology, Thataguni, Off Kanakapura Road, Bangalore, Karnataka, 560082, India

## ARTICLE INFO

### Keywords:

Banana corm extract  
Microwave  
ZnO  
Fish lipid  
Transesterification  
Biodiesel

## ABSTRACT

This paper reports the green way of zinc oxide synthesis using the aqueous extract of the corm (rhizome) of the banana plant (*Musa spp.*) via an eco-friendly microwave approach. Zinc oxide catalysts were prepared in a different molar concentration of ZnSO<sub>4</sub>·7H<sub>2</sub>O solutions (0.1–0.5 M) and different volume of banana corm extract (16 mg/ml; 1–5 ml). The aqueous extract of banana corm plays a role of reducing agents and stabilizer. The synthesized zinc oxide catalyst was characterized by instrumental techniques such as UV–Vis spectroscopy, XRD, FT-IR, DLS and SEM micrograph. The obtained results have confirmed the creation of sphere-shaped/globular zinc oxide with an average particle size of ~370 nm. The varied amount of zinc oxide catalyst (2–3 wt. %) was used for the transesterification of fish lipid into biodiesel. The prepared biodiesel was examined via <sup>1</sup>H NMR spectroscopy and GC-MS. The maximum transesterification efficiency was found to be ~90% for the ZnO catalyst at 2.5 wt %. The banana corm extracts (BCE) mediated synthesis of ZnO catalyst has shown for its potential application for sustainable biodiesel development.

## 1. Introduction

The rise in energy demands, exploitation of fossil fuel assets and ecological alarms impules the development of alternative renewable energy resources for sustainability. The renewable and eco-friendly transport fuel *i.e.* biodiesel incited much attention for transportation/industrial sector due to the several benefits. Chemically, the biodiesel is the methyl esters of fatty acids (FAME) which can be obtained from animal fats/lipids or edible/non-edible oils via its transesterification. Biodiesel is an environment-friendly fuel to substitute the petrodiesel for direct use or to blend with petrodiesel (Baskar and Aiswarya, 2015; Talebian-Kiakalaieh et al., 2013; Jaiswal and Arun Prasath, 2016).

The variety of feedstock resources from plant or animal origin can be employed to manufacture the biodiesel. The low-cost, non-edible or waste resources for the feedstock are also in the audience to avoid the discussion over ‘food’ vs. ‘fuel’ concern (David, 2008). In the waste

resources, discarded fish waste attracted much attention as a potential feedstock in biodiesel production. The fishery trades explore huge commercial and nutritional significance in India and abroad. India contributes as the second top in the world with ~5.5% of the worldwide production of fish owing longest sea shoreline ~8000 km and inland fisheries (Venkataraman, 2012). The fish processing industry and marketplace produce huge amounts of fish cast-off/waste (head, viscera, tail, skin, liver, eyes, fins, etc.) about 1/3rd portion. The extracted crude oil from the waste parts of marine/freshwater fish can be deliberated to be a substitute resource of low-cost feedstock to produce biodiesel due to high contents of long-chain fatty acids (Jaiswal et al., 2014). The lipids/fats obtained from waste fish has to undergo for transesterification reaction to produce biodiesel.

The reaction for biodiesel synthesis *i.e.* transesterification can be catalyzed via a wide range of catalysts such as homogeneous, heterogeneous or enzymatic catalysts under appropriate reaction condition.

\* Corresponding author.

E-mail address: [raprasath.get@pondiuni.edu.in](mailto:raprasath.get@pondiuni.edu.in) (A.P. Ramaswamy).

<sup>1</sup> Authors for equal contributions.

**Table 1**  
Synthesis of ZnO using a varied concentration of BCE and ZnSO<sub>4</sub>·7H<sub>2</sub>O solution.

S. No.	Banana Corm Extract (ml)	ZnSO <sub>4</sub> ·7H <sub>2</sub> O (Molar)	Time (min)	Microwave Irradiation Power (Watt)
1.	1 ml	0.1 M	15	P-60 (540 Watt)
2.	1 ml	0.2 M	15	P-60 (540 Watt)
3.	1 ml	0.3 M	15	P-60 (540 Watt)
4.	1 ml	0.4 M	15	P-60 (540 Watt)
5.	1 ml	0.5 M	15	P-60 (540 Watt)
6.	2 ml	0.2 M	15	P-60 (540 Watt)
7.	3 ml	0.2 M	15	P-60 (540 Watt)
8.	4 ml	0.2 M	15	P-60 (540 Watt)
9.	5 ml	0.2 M	15	P-60 (540 Watt)
10.	0 ml	0.2 M	15	P-60 (540 Watt)

Traditional homogeneous catalysts have several drawbacks including the sensitivity to free fatty acid which marks the formation of soap, whereas enzyme catalysts showed its limitation such as high cost, slower reaction rate and deactivation by alcohol used as acyl acceptor (Wilson and Lee, 2012). In this perspective, heterogeneous catalyst inclines to conquer the limitations with the homogeneous and enzymatic catalysts. Heterogeneous catalysts have shown its potentials in the line of transesterification of low-grade oil with fewer purification steps, mild reaction condition and easy separation. Numerous heterogeneous catalysts e.g. hydrotalcite, alkali oxides, metal oxides, etc. are well reported to be used for the biodiesel synthesis (Helwani et al., 2009; Lee et al., 2014; Jha et al., 2016).

In addition, numerous investigation on the synthesized nanomaterials/composites are reported such as metal oxides (ZnO, CaO, MgO, Ca/Zn, Ca/Mg, etc.), alkali metal oxides (CaO/Al<sub>2</sub>O<sub>3</sub>, MgO/Al<sub>2</sub>O<sub>3</sub>, Li/CaO, etc.), hydrotalcite, Ca/Al/Fe<sub>3</sub>O<sub>4</sub> magnetic composites, polymeric composites, graphene-based materials and biologically derived catalysts to be utilized in catalytic activity and reusability for biodiesel production process (Lee et al., 2014; Jha et al., 2016; Jaiswal et al., 2018a, 2018b; Sudhakar, 2018; Sudhakar et al., 2017). The various parameters e.g. temperature, oil to methanol ratio, reaction time and catalyst concentration are considered for transesterification. The heterogeneous catalysts of metal oxides contain positive metal ions (electron acceptors) and negative oxygen ions (proton acceptors). The electron and proton acceptors offer adsorptive sites for methanol and readily split in the anions of methoxide as well as cations of hydrogen. The methoxide anions of the heterogeneous catalysts react with the triglyceride of lipid to convert into methyl ester (Sharma et al., 2011). Recently, low-cost and efficient catalysts such as bio-derived transition metal oxides (e.g. CaO, ZnO, MgO, SiO<sub>2</sub>, etc.) are gaining interest due to the ease of synthesis, non-toxicity and wide range applicability including transesterification reaction (Baskar et al., 2018). Among the variety of agro-waste materials, leftovers of banana plant considered as one of the highly abundant agro-waste (Padam et al., 2014). The phytochemicals in the extracts have the potential to act as reducing agents and a stabilizer to synthesize metal/metal oxide nanomaterials via green and environment-friendly approach for various applications (Padam et al., 2014; Dauthal and Mukhopadhyay, 2016).

In this study, transition metal oxide ZnO heterogeneous catalyst was prepared by the mediation of aqueous extract of the banana corm (BCE) under the microwave irradiation. The synthesized ZnO catalyst was utilized for the biodiesel synthesis via transesterification reaction and the conversion efficiency of lipid into FAME was investigated in different concentration of biologically synthesized ZnO.

## 2. Experimental

### 2.1. Materials

Corms (rhizome) of banana plant (*Musa spp.*) were collected from the village Poornankuppam of Ariyankuppam Commune, Puducherry, India

(11.865839°N 79.805288°E). Discarded fish wastes (leftover of fish e.g. head, tail, skin, viscera, etc.) were collected from the fish market of Kalapet, Puducherry, India (12°2'4.93"N 79°51'52.24"E).

Zinc sulphate heptahydrate (ZnSO<sub>4</sub>·7H<sub>2</sub>O), chloroform, methanol, ethanol and ethylene glycol were procured from Merck Chemicals, India. Potassium bromide (KBr) and deuterated chloroform (CDCl<sub>3</sub>) were purchased from Sigma-Aldrich, India. Milli-Q water was used for the preparation of plant extract.

### 2.2. Preparation of aqueous extract from the corm (rhizome) of the banana plant

The freshly collected corm (rhizome) of the banana plant was cleaned numerous times with water followed by distilled water to eliminate soil and other impurities. The banana corm was sliced into small pieces and dried in shade. The dried banana corm was ground into a fine powder using an electric household grinder. The powdered banana corm was added in Milli-Q in the ratio of 1:10 and kept for stirring at 60 °C for 45 min. Then, the aqueous solution was centrifuged at 10000 rpm for 15 min and separated supernatant was filtered using Whatman Filter Paper No. 1. Banana corm extract (16 mg/ml) was kept at ambient room temperature for further usage.

### 2.3. Synthesis of ZnO under microwave irradiation using BCE

The preparation of ZnO catalyst was optimized with banana corm extract (16 mg/ml; 1–5 ml) mixed with a different molar concentration of ZnSO<sub>4</sub>·7H<sub>2</sub>O (0.1–0.5 M) solutions and stirred vigorously at 80 °C (see Table 1). The resultant solutions were treated under microwave irradiation at P-60 (540 Watt) for 15 min in a domestic microwave. The microwave treated solution turns brownish-white in colour indicating the synthesis of product. The synthesized products were washed several times using Milli-Q water followed by ethanol. The obtained product was kept in a furnace for calcination at 400 °C for 3 h to remove unreacted/impurities.

### 2.4. Materials characterization

The preparation of ZnO with the aqueous extract of the banana corm was characterized using UV-VIS-NIR Spectrometer in the range of 200–800 nm. The phase purity and lattice parameter of the synthesized ZnO catalyst was analyzed by X-ray diffractometer (X'Pert PRO, PAN-analytical) with Cu K $\alpha$  radiation ( $\lambda = 1.5406 \text{ \AA}$ ) in the range 15–80° with the step size of 0.015°. Infrared spectra (400–4000 cm<sup>-1</sup>) of the samples were recorded by Fourier transform infrared spectrometer (Make: Thermo Nicolet, Model: 6700) using KBr pellet technique. The size of ZnO was measured by dynamic light scattering (Malvern Panalytical, MAL1043157). The surface configuration of the synthesized ZnO was characterized by SEM (scanning electron microscope) micrograph (Make: Hitachi, Model: S-3400N).

### 2.5. Biodiesel synthesis from fish lipids and analysis

The discarded fish wastes/residues were collected from the local fish market at Kalapet, Puducherry. The fish waste was kept for drying in an oven at 60 °C and ground into the fine powder, and subsequently, the lipid extraction was carried out by the Folch's method (Folch et al., 1957). The extracted and purified fish lipids were used for transesterification. The purified fish lipid was preheated at 70 °C to remove moisture from the lipids. The synthesized ZnO catalysts (2–3 wt. %) was mixed in fish lipids and stirred for a few minutes to make it slurry and, successively methanol was added and allowed to stir continuously with a mechanical stirrer until the transesterification reaction. The reaction conditions for transesterification were 6:1 ratio of methanol to lipids at 70 ± 2 °C for 4 h. The biodiesel phase at the top layer was separated by centrifuge at 2000 rpm for 15 min; subsequently, a hot water

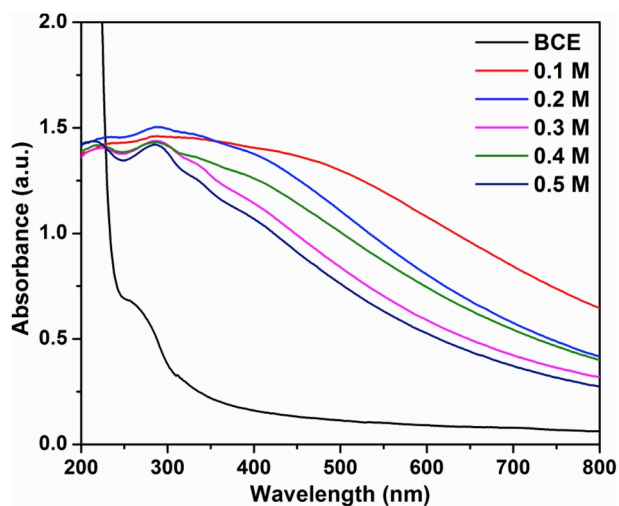


Fig. 1. UV-Vis spectra of ZnO synthesis at varied  $\text{ZnSO}_4 \cdot 7\text{H}_2\text{O}$ .

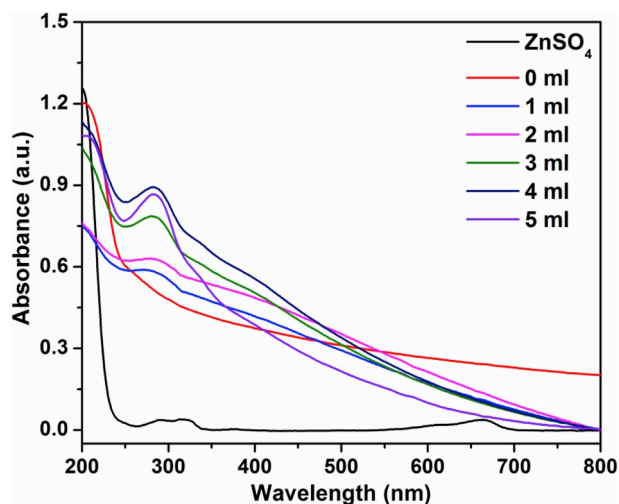


Fig. 2. UV-Vis spectra of ZnO synthesis at varied BCE.

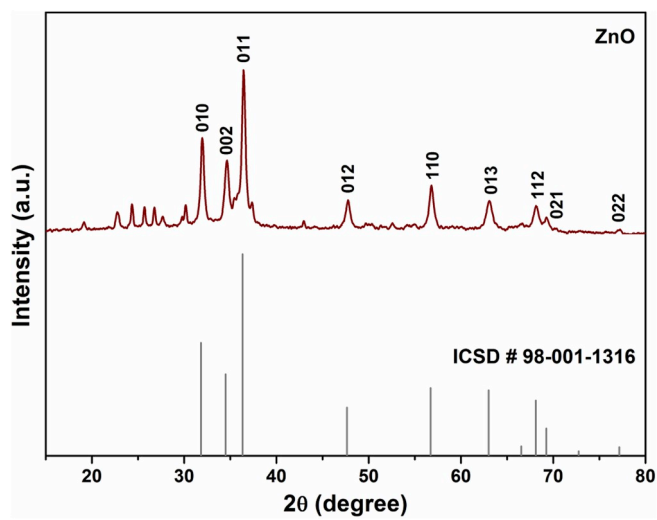


Fig. 3. XRD pattern of ZnO catalyst.

Table 2

FT-IR Spectral peaks of banana corm powder, banana corm extract and synthesized ZnO.

S. No.	Absorption peak ( $\text{cm}^{-1}$ )	Bond/functional groups
1.	3441	OH stretching vibrations
2.	2991	C-H stretching band vibration
3.	1648	C=C stretch in aromatic ring and $\text{C}=\text{O}$ stretch in polyphenols
4.	1388	C-H bending alkane group
5.	1270	C-N stretching of the amine group
6.	1040	C-O stretching in amino acid
7.	476	The hexagonal phase of ZnO stretching band

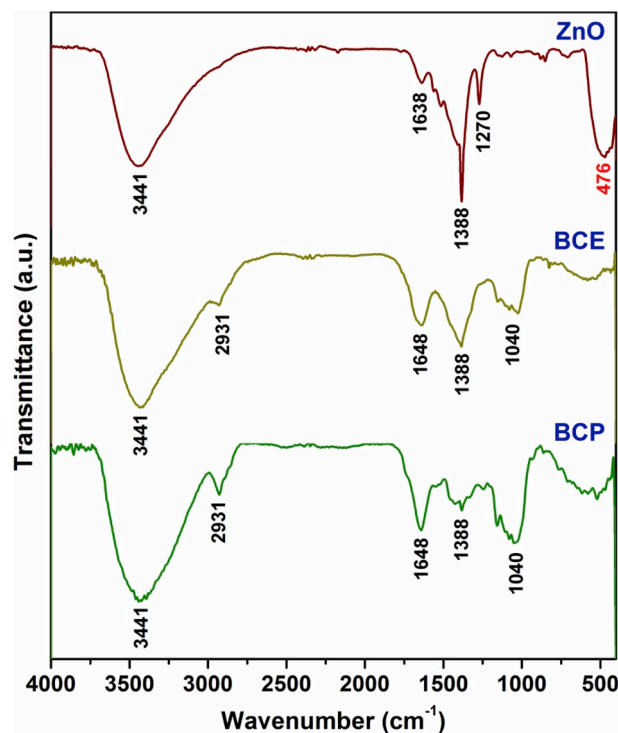


Fig. 4. FTIR spectra of optimized ZnO catalyst, BCE and BCP.

purification step was carried out. The transformation of lipids to biodiesel was calculated by  $^1\text{H}$  NMR spectroscopy using the ratio of integrated signals (area under the signal acquired by integration) at 3.68 ppm ( $A_{\text{CH}_3}$ ) and at 2.28 ppm ( $A_{\text{CH}_2}$ ). The content of fatty acids methyl esters (FAME) was analyzed by GC-MS using instrument acquisition parameters; oven: initial temp  $60^\circ\text{C}$  for 2.80 min, ramp  $10^\circ\text{C}/\text{min}$  to  $300^\circ\text{C}$ , hold 6 min, InjAauto  $260^\circ\text{C}$ , volume  $0\ \mu\text{L}$ , split 10:1, carrier gas He, solvent delay 2.80 min, transfer temp  $225^\circ\text{C}$ , source temp  $225^\circ\text{C}$ , scan: 40 to 600Da, column  $30.0\text{m} \times 250\ \mu\text{m}$ .

### 3. Results and discussion

#### 3.1. UV-Vis spectroscopy of ZnO synthesis

Fig. 1 represents the optical absorbance spectra for the blank BCE (16 mg/ml) and BCE mediated synthesis of ZnO using a different molar concentration of  $\text{ZnSO}_4 \cdot 7\text{H}_2\text{O}$  (0.1–0.5 M) solution. The typical exciton absorption peak of blank banana corm extract (BCE) was observed at 252 nm which was shifted at 288 nm during the synthesis of ZnO using a different molar concentration of the solutions of  $\text{ZnSO}_4 \cdot 7\text{H}_2\text{O}$ . The increase in molar concentration of the solutions of  $\text{ZnSO}_4 \cdot 7\text{H}_2\text{O}$  increases the absorbance peak intensity at 0.2 M and then after decreases from

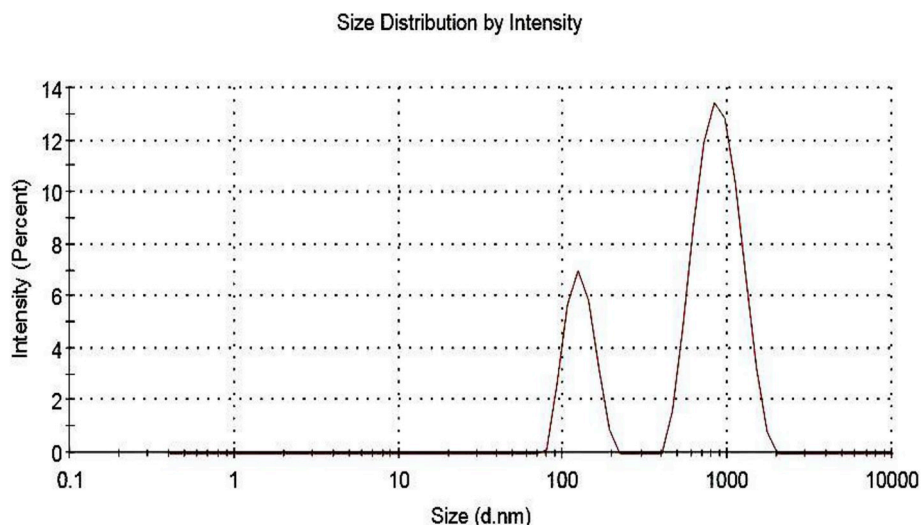


Fig. 5. DLS of ZnO catalyst.

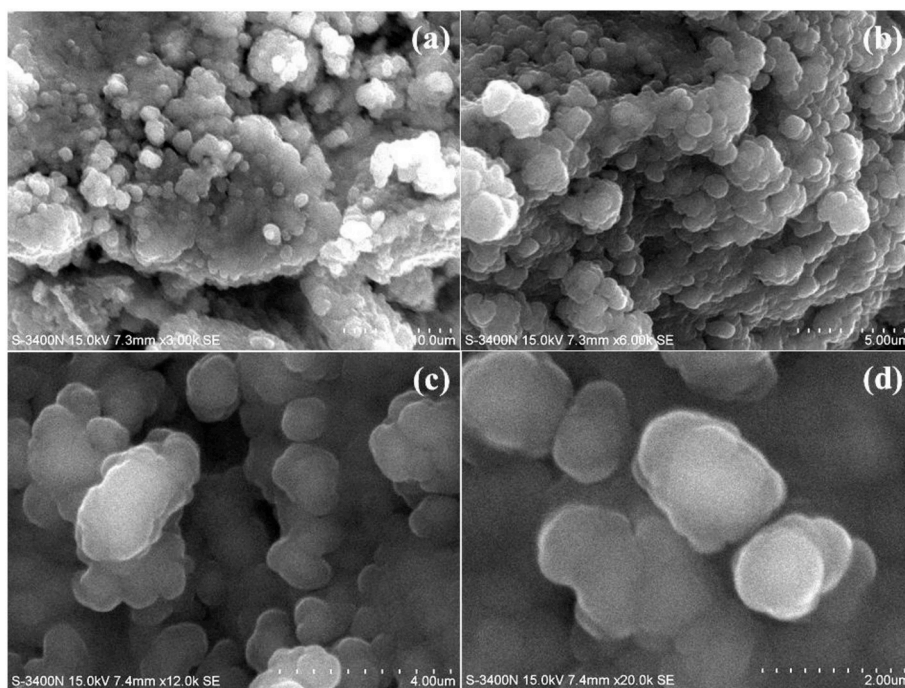


Fig. 6. SEM micrograph of ZnO catalyst.

0.3–0.5 M concentrations (Fig. 1).

In Fig. 2, the optical absorbance spectra for the blank  $\text{ZnSO}_4 \cdot 7\text{H}_2\text{O}$  solution and BCE mediated synthesis of ZnO in the varied volume of BCE (0–5 ml) has shown. The typical exciton absorption peak of blank  $\text{ZnSO}_4 \cdot 7\text{H}_2\text{O}$  solution was observed at 320 nm which was shifted towards at 288 nm during the synthesis of ZnO using varied volume concentration of BCE. It was observed that without using BCE (0 ml) in  $\text{ZnSO}_4 \cdot 7\text{H}_2\text{O}$  solution, there is no indication for the formation of ZnO as shown in the spectra of Fig. 2. The absorption peak intensity increases with an increase in volume with a decrease at 4 ml concentration as optimum (Fig. 2). The absorption edge intensity in volume optimization shows a systematic shift towards the lower wavelength or higher energy (blue shift) at 282 nm compared to 288 nm which indicates the reduction in particles size of biologically synthesized ZnO catalysts (Dobrucka and Dugaszewska, 2016). The optimized sample synthesized ZnO using 4 ml BCE and 0.2 M  $\text{ZnSO}_4 \cdot 7\text{H}_2\text{O}$  solution were used for further

instrumental characterization and as catalysts in the transesterification reaction.

### 3.2. X-ray diffraction of biologically synthesized ZnO catalyst

The XRD pattern of BCE mediated biologically synthesized ZnO catalyst and standard ICSD reference has presented in Fig. 3. The corresponding diffraction peaks at  $31.8^\circ$  (0 1 0),  $34.5^\circ$  (0 0 2),  $36.3^\circ$  (0 1 1),  $47.6^\circ$  (0 1 2),  $56.7^\circ$  (1 1 0),  $63.0^\circ$  (0 1 3),  $66.5^\circ$  (0 2 0),  $68.1^\circ$  (1 1 2),  $69.2^\circ$  (0 2 1) and  $77.1^\circ$  (0 2 2) attributed to the indexing planes of ZnO, signifying the hexagonal crystal system (ICSD Card No.: 98-001-1316) (Bi et al., 2017). The crystallite size was calculated 14.64 nm using highest intensity peaks (Full width at half maximum (0 1 1)  $0.596^\circ$  and peak position  $36.447^\circ$ ) for the synthesized ZnO by Debye-Scherrer equation [Crystallite size (D) =  $K\lambda/(\beta \cos \theta)$ ].

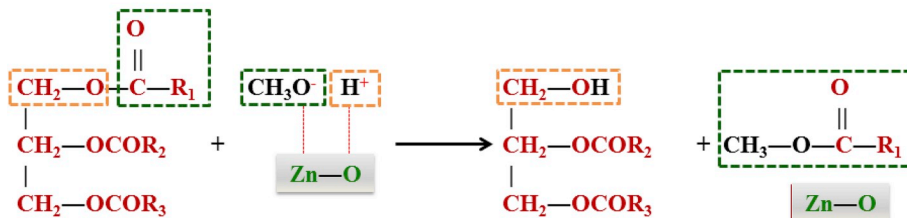
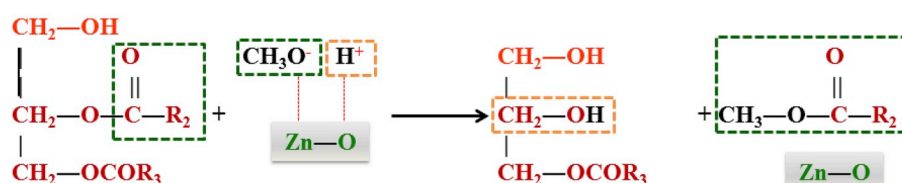
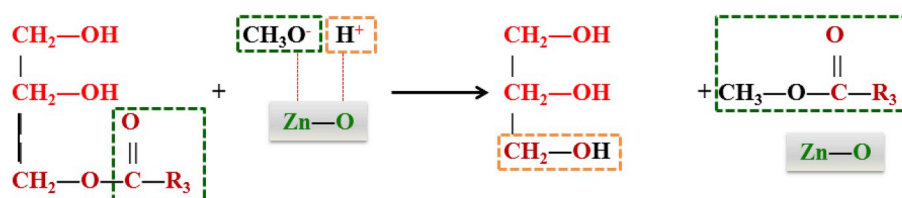
**Step I****Step II****Step III****Step IV**

Fig. 7. Proposed transesterification reaction mechanism of fish lipid using ZnO catalyst.

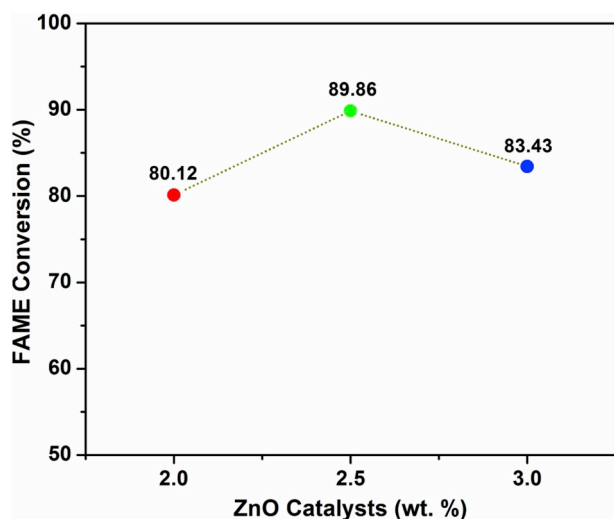


Fig. 8. FAME conversion efficiency at a varied amount of ZnO catalysts.

**3.3. Fourier-transform infrared spectroscopy of synthesized ZnO catalyst**

The IR spectrum of the optimized ZnO catalyst, BCE and BCP (banana corm powder) has represented in Table 2 and Fig. 4. The characteristics absorption band vibration at  $476\text{ cm}^{-1}$  corresponds to the Zn-O

stretching band vibration. The vibration band in the fingerprint region at  $1382\text{ cm}^{-1}$  signifies the stretching band of C-H and at the  $1638\text{ cm}^{-1}$  denotes C=C as well as C=O stretching vibration of functional groups, which indicates the presence of organic species of corn extract. The additional peaks at  $3441\text{ cm}^{-1}$  attributes the stretching vibration and bending mode of O-H group appears due to for adsorbed water molecules. The remaining band vibrations ascribed to organic impurities originating from the root extract mediated synthesis of ZnO catalyst (Suresh et al., 2018; Rengasamy et al., 2016).

**3.4. Dynamic light scattering spectroscopy of biologically synthesized ZnO catalyst**

The particle size of the biologically synthesized ZnO catalyst was analyzed by DLS spectroscopy as represented in Fig. 5. It was observed that most of the sizes of particles were in varied range. The average particle size distribution (Z-Average) was recorded as 372 nm (Geetha Devi and Sakthi Velu, 2016).

**3.5. Scanning electron microscopy of synthesized ZnO catalyst**

The SEM micrograph of synthesized optimized ZnO has represented in Fig. 6 (a, b, c and d). The micrograph shows the formation of a sphere-shaped/globular structure of ZnO catalyst with varied sizes (Fig. 5 a and b). It is clearly observed that the agglomeration had been taken place. The higher magnification of SEM images has shown the presence of agglomeration in the sample (Fig. 6 c and d). The XRD pattern and FTIR

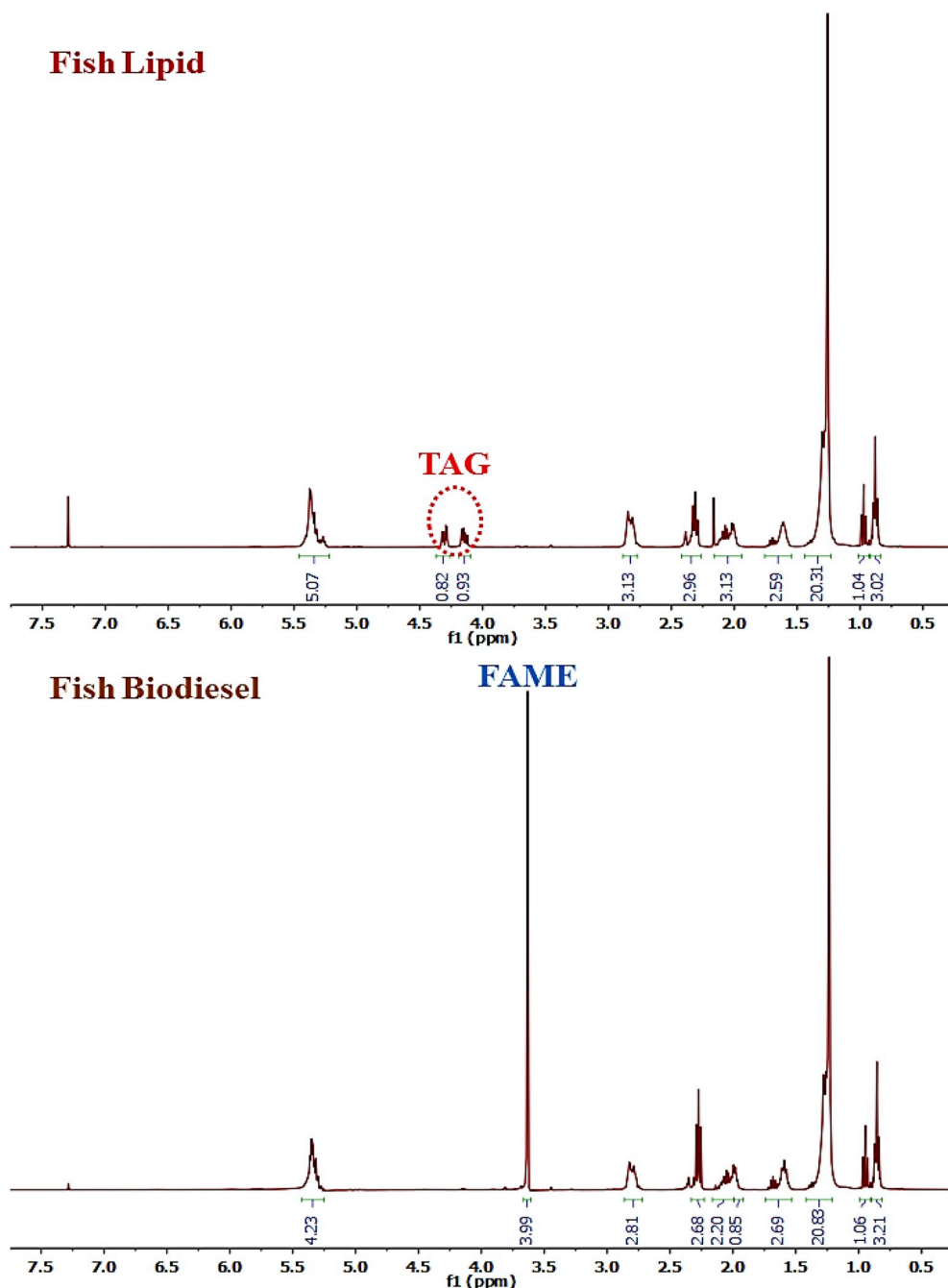


Fig. 9.  $^1\text{H}$  NMR of fish lipid and fish biodiesel.

**Table 3**

FAME conversion at different concentration of ZnO catalysts.

S. No.	ZnO Catalyst (wt. %)	$A_{CH_3}$ (ppm)	$A_{CH_2}$ (ppm)	FAME Conversion (%)
1.	2.0	2.56	2.13	80.12
2.	2.5	3.99	2.96	89.86
3.	3.0	1.99	1.59	83.43

spectrum support the synthesized particles as biologically synthesized ZnO.

### 3.6. Active component and transesterification reaction mechanism of the ZnO catalyst

The proposed transesterification reaction mechanism of fish lipid

using ZnO catalysts is indicated in Fig. 7. The transesterification reaction of fish lipid with methanol was performed at  $70 \pm 2^\circ\text{C}$  for 4 h to obtain biodiesel (FAME) and glycerol. The biologically synthesized ZnO acted as a catalyst in the transesterification of fish lipid. In the proposed transesterification reaction mechanism, in step I, the ZnO catalysts show the transfer of a proton from methanol to form a methoxide anion. In step II, the carbonyl carbon of the triglycerides of the fish lipid was reacted with the methoxide anion to form 1 mol of FAME and 1 mol of diglyceride through the intermediate methoxycarbonyl. Similarly, step III and IV followed the process to form FAME from diglyceride and monoglyceride formed during the transesterification reaction (Rengasamy et al., 2016; Geetha Devi and Sakthi Velu, 2016). As a final point, 1 mol of triglyceride reacted with the 3 mol of methanol to form 3 mol of respective FAME (biodiesel) and 1 mol of glycerol byproduct from fish lipid.

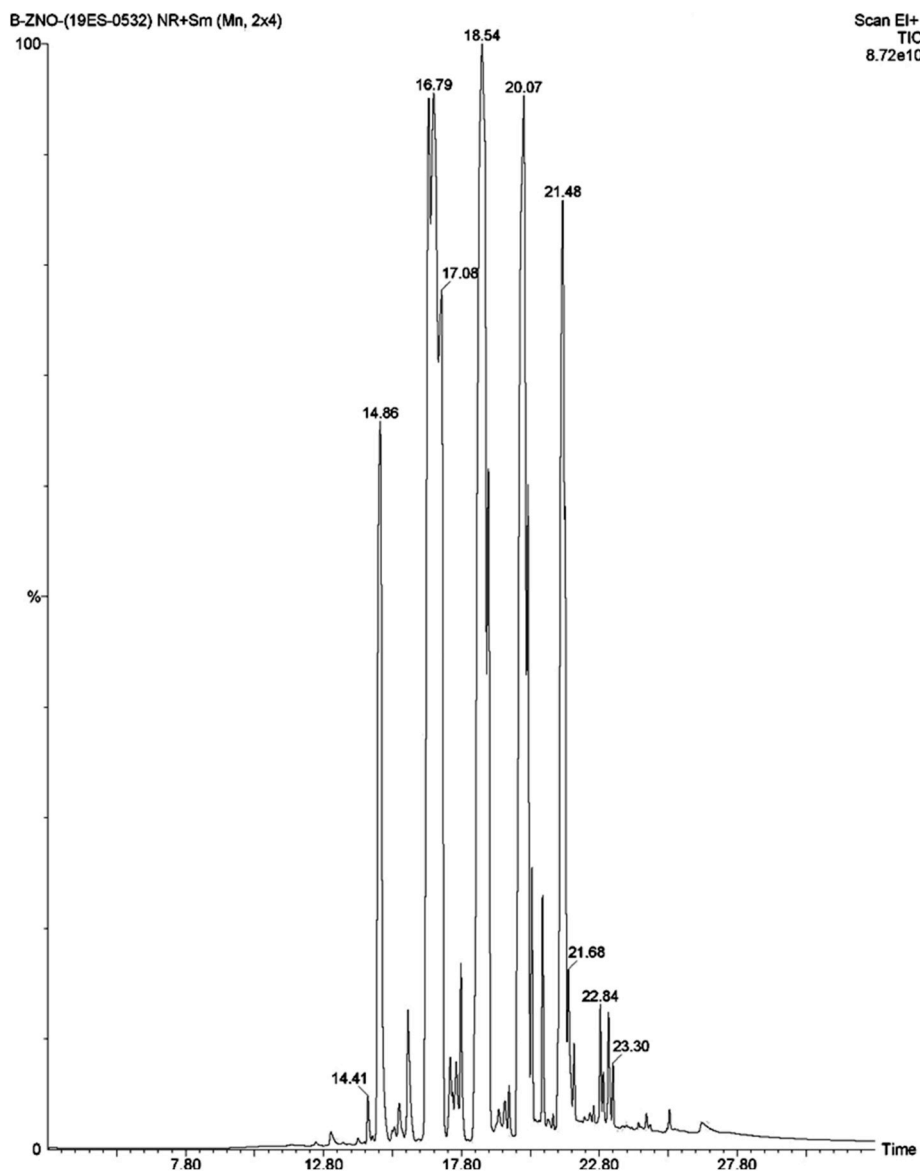


Fig. 10. GC-MS chromatogram of fish biodiesel.

### 3.7. $^1\text{H}$ NMR spectroscopy of fish lipid and fish biodiesel

The conversion of fish lipid into the biodiesel (FAME) was analyzed via  $^1\text{H}$  NMR spectroscopy and the recorded spectra are represented in Fig. 9. A strong singlet signal at 3.68 ppm designates methoxy proton of methyl ester ( $-\text{CO}_2\text{CH}_3$ ) formation of FAMES, while triplets at 2.28 ppm denote  $\alpha$ -methylenes proton of fatty acid derivatives. The disappearance of the signal at 4.14–4.33 ppm in the fish biodiesel sample indicates the disappearance of the proton attached to the glycerol moiety of mono-, di-, or triacylglycerols. The conversion of lipids to biodiesel was estimated by  $^1\text{H}$  NMR spectroscopy using the ratio of integrated signals (area under the signal obtained by integration) at 3.68 ppm ( $A_{\text{CH}_3}$ ) and at 2.28 ppm ( $A_{\text{CH}_2}$ ) using equation  $[C = 100 (2 \times A_{\text{CH}_3}) / (3 \times A_{\text{CH}_2})]$  (Madhu et al., 2017).

The aim to determine the optimized amount of catalyst with fixed reaction parameters for transesterification has revealed that the 2.5 wt % of biologically synthesized ZnO has higher efficiency of transesterification conversion (Fig. 8). It was observed that as the amount of the catalyst increases from 2.0–2.5 wt %, the conversion efficiency increased while increasing amount of catalyst from the 2.5–3.0 dropped the conversion efficiency (Table 3). Consequently, it can be assumed

that the optimized amount of catalyst ensured the fastest transesterification reaction rates for the studied parameters.

### 3.8. GC-MS of fish biodiesel

The synthesized biodiesel from fish lipid was analyzed by GC-MS and represented in the chromatogram (Fig. 10). The constituents were predicted by NIST library matching as shown in Table 4. The analysis of fish biodiesel shown the presence of FAME constituents viz. 5-hydroxy-2,4-dimethylpentanoic acid methyl ester ( $\text{C}_8\text{H}_{16}\text{O}_3$ ), pentadecanoic acid methyl ester ( $\text{C}_{16}\text{H}_{32}\text{O}_2$ ), 9-hexadecenoic acid methyl ester ( $\text{C}_{17}\text{H}_{32}\text{O}_2$ ), 13-docosenoic acid methyl ester ( $\text{C}_{23}\text{H}_{44}\text{O}_2$ ), ethyl 13-methyl-tetradecanoic acid methyl ester ( $\text{C}_{17}\text{H}_{34}\text{O}_2$ ), hexacosanoic acid methyl ester ( $\text{C}_{27}\text{H}_{54}\text{O}_2$ ), 9-octadecenoic acid methyl ester ( $\text{C}_{19}\text{H}_{36}\text{O}_2$ ), 2-methyl-tetradecanoic acid methyl ester ( $\text{C}_{16}\text{H}_{32}\text{O}_2$ ), 10,13-octadecadiynoic acid methyl ester ( $\text{C}_{19}\text{H}_{30}\text{O}_2$ ), eicosanoic acid methyl ester ( $\text{C}_{21}\text{H}_{42}\text{O}_2$ ), Cis-5,8,11,14,17-eicosapentaenoic acid methyl ester ( $\text{C}_{21}\text{H}_{32}\text{O}_2$ ), 9,12-octadecadiynoic acid methyl ester ( $\text{C}_{19}\text{H}_{30}\text{O}_2$ ) and 10,13-octadecadiynoic acid methyl ester ( $\text{C}_{19}\text{H}_{30}\text{O}_2$ ) (Madhu et al., 2017).

**Table 4**  
Main composition of FAMES in fish biodiesel.

S. No.	RT	Composition (%)	Formula	Compound Name (FAME)
1.	14.883	8.443	C <sub>8</sub> H <sub>16</sub> O <sub>3</sub>	5-hydroxy-2,4-dimethylpentanoic acid methyl ester
2.	15.849	0.853	C <sub>16</sub> H <sub>32</sub> O <sub>2</sub>	Pentadecanoic acid methyl ester
3.	16.619	9.929	C <sub>17</sub> H <sub>32</sub> O <sub>2</sub>	9-hexadecenoic acid methyl ester
4.	16.804	17.287	C <sub>23</sub> H <sub>44</sub> O <sub>2</sub>	13-docosenoic acid methyl ester
5.	17.079	10.856	C <sub>17</sub> H <sub>34</sub> O <sub>2</sub>	Ethyl 13-methyl-tetradecanoic acid methyl ester
6.	17.774	0.756	C <sub>27</sub> H <sub>54</sub> O <sub>2</sub>	Hexacosanoic acid methyl ester
7.	18.530	23.925	C <sub>19</sub> H <sub>36</sub> O <sub>2</sub>	9-octadecenoic acid methyl ester
8.	18.800	4.600	C <sub>16</sub> H <sub>32</sub> O <sub>2</sub>	2-methyl-tetradecanoic acid methyl ester
9.	20.100	8.128	C <sub>19</sub> H <sub>30</sub> O <sub>2</sub>	10,13-octadecadiynoic acid methyl ester
10.	20.365	1.149	C <sub>21</sub> H <sub>42</sub> O <sub>2</sub>	Eicosanoic acid methyl ester
11.	20.746	0.934	C <sub>21</sub> H <sub>32</sub> O <sub>2</sub>	Cis-5,8,11,14,17-eicosapentaenoic acid methyl ester
12.	21.481	8.532	C <sub>19</sub> H <sub>30</sub> O <sub>2</sub>	9,12-octadecadiynoic acid methyl ester
13.	21.576	2.574	C <sub>19</sub> H <sub>30</sub> O <sub>2</sub>	10,13-octadecadiynoic acid methyl ester

#### 4. Conclusion

The ZnO catalyst was successfully prepared *via* green approaches with the aqueous extract of banana corm *via* microwave irradiation. The structural analysis of the optimized sample was characterized *via* XRD which confirmed the phase presence of hexagonal crystal system of ZnO with crystallinity 14.64 nm. FTIR spectroscopy coincides the characteristics of stretching band vibration for Zn–O at 476 cm<sup>-1</sup>. The average particles size found to be 372 nm by DLS spectroscopy. The SEM micrograph of ZnO represented a sphere-shaped/globular with a varied size range. The biologically synthesized ZnO catalysts were used to produce biodiesel from fish lipid. The transesterification conversion efficiency of fish lipid to biodiesel was calculated *via* <sup>1</sup>H NMR spectroscopy studies and found to be the highest 89.86% with ZnO catalyst (2.5 wt %). The GC-MS has confirmed the main constituents of FAME in fish biodiesel. The study represents the potential transesterification of lipid for sustainable biodiesel production.

#### Acknowledgments

The authors are grateful to acknowledge the Central Instrumental Facility (CIF), Pondicherry University, Puducherry for characterization facilities. We are also grateful to the Sophisticated Instrumentation Facility, VIT University, Vellore, Tamil Nadu for GCMS analysis and Center for Incubation, Innovation, Research and Consultancy, Jyothy Institute of Technology, Bangalore, Karnataka for XRD characterization.

#### References

Baskar, Gurunathan, Aiswarya, Ravi, 2015. Biodiesel production from waste cooking oil using copper doped zinc oxide nanocomposite as heterogeneous catalyst. *Bioresour. Technol.* 188, 124–127p.

- Baskar, G., Aberna Ebenezer Selvakumari, I., Aiswarya, R., 2018. Biodiesel production from castor oil using heterogeneous Ni doped ZnO nanocatalyst. *Bioresour. Technol.* 250, 793–798p.
- Bi, Chongyao, Li, Jianwei, Peng, Lijun, Zhang, Jianmin, 2017. Biofabrication of Zinc oxide nanoparticles and their in-vitro cytotoxicity towards gastric cancer (MGC803) cell lines. *Biomed. Res.* 28 (5), 2065–2069p.
- Dauthal, Preeti, Mukhopadhyay, Mausumi, 2016. Noble metal nanoparticles: plant-mediated synthesis, mechanistic aspects of synthesis, and applications. *Ind. Eng. Chem. Res.* 55, 9557–9577p.
- David, J., 2008. Tenenbaum. *Food vs. Fuel: diversion of crops could cause more hunger.* *Environ. Health Perspect.* 116 (6), A254–A257p.
- Dobrucka, Renata, Dugaszweska, Jolanta, 2016. Biosynthesis and antibacterial activity of ZnO nanoparticles using *Trifolium pratense* flower extract. *Saudi J. Biol. Sci.* 23, 517–523p.
- Folch, Jordi, Lees, M., Stanley, G. H. Sloane, 1957. A simple method for the isolation and purification of total lipids from animal tissues. *J. Biol. Chem.* 226, 497–509p.
- Geetha Devi, P., Sakthi Velu, A., 2016. Structural and optical properties of pure ZnO and Co doped ZnO nanoparticles prepared by the co-precipitation method. *J. TheorAppl Phys* 10, 233–240p.
- Helwani, Z., Othman, M.R., Aziz, N., Kim, J., Fernando, W.J.N., 2009. Solid heterogeneous catalysts for transesterification of triglycerides with methanol: a review. *Appl. Catal. Gen.* 363 (1–2), 1–10p.
- Jaiswal, K.K., Arun Prasath, R., 2016. Integrated growth potential of *Chlorella pyrenoidosa* using hostel mess wastewater and its biochemical analysis. *Int. J. Environ. Sci.* 6 (5), 592–599p.
- Jaiswal, K.K., Jha, B., Arun Prasath, R., 2014. Biodiesel production from discarded fish waste for sustainable clean energy development. *J. Chem. Pharm. Sci.* 4, 113–114p. Special Issue.
- Jaiswal, Krishna Kumar, Manikandan, Dhamodaran, Murugan, Ramaswamy, Ramaswamy, Arun Prasath, 2018. Microwave-assisted rapid synthesis of Fe<sub>3</sub>O<sub>4</sub>/poly(styrene-divinylbenzeneacrylic acid) polymeric magnetic composites and investigation of their structural and magnetic properties. *Eur. Polym. J.* 98, 177–190p.
- Jaiswal, Krishna Kumar, Sudhakar, S., Ramaswamy, Arun Prasath, 2018. 'Graphene'-World's thinnest material for revolutionizing applications. *Everyman's Science LIII* (4), 219–223p.
- Jha, Bhaskar, Jaiswal, Krishna Kumar, Ramaswamy, Arun Prasath, 2016. Impact of poly-aluminium chloride on foam suppression in a chicken waste based biogas plant: a case study at KEPCO Kerala. *Int. J. Environ. Sci.* 6 (6), 934–940p.
- Lee, Adam F., Bennett, James A., Manayil, Jinesh C., Wilson, Karen, 2014. Heterogeneous catalysis for sustainable biodiesel production via esterification and transesterification. *Chem. Soc. Rev.* 43, 7887–7916p.
- Madhu, Devarapaga, Arora, Rajan, Sahani, Shalini, Singh, Veena, Sharma, Yogesh Chandra, 2017. Synthesis of high-quality biodiesel using feedstock and catalyst derived from fish wastes. *J. Agric. Food Chem.* 65, 2100–2109.
- Padam, Birdie Scott, Tin, Hoe Seng, Chye, Fook Yee, Abdullah, Mohd Ismail, 2014. Banana by-products: an under-utilized renewable food biomass with great potential. *J. Food Sci. Technol.* 51 (12), 3527–3545p.
- Rengasamy, Mookan, Anbalagan, Krishnasamy, Kodhaiyolii, Shanmugam, Pugalanthi, Velan, 2016. Castor leaves mediated synthesis of iron nanoparticles for evaluating catalytic effects in transesterification of castor oil. *RSC Adv.* 6, 9261–9269p.
- Sharma, Yogesh C., Singh, Bhaskar, Korstad, John, 2011. Latest developments on application of heterogeneous basic catalysts for an efficient and ecofriendly synthesis of biodiesel: a review. *Fuel* 90, 1309–1324p.
- Sudhakar, S., 2018. Krishna kumar jaiswal, Arun Prasath ramaswamy. The role of microwave irradiation temperature on nitrogen doping in metal-free graphene catalysts for an efficient oxygen reduction reaction in an alkaline condition. *ChemistrySelect* 3, 8962–8972p.
- Sudhakar, S., Jaiswal, Krishna Kumar, Gouse Peera, S., Ramaswamy, Arun Prasath, 2017. Green synthesis of n-graphene by hydrothermal-microwave irradiation for alkaline fuel cell application. *Int. J. Recent. Sci.Res.* 8 (8), 19049–19053p.
- Suresh, Joghhe, Pradheesh, Ganeshan, Vincent, Alexramani, Sundrarajan, Mahalingam, Sun, Ig Hong, 2018. Green synthesis and characterization of zinc oxide nanoparticle using insulin plant (*Costus pictus* D. Don) and investigation of its antimicrobial as well as anticancer activities. *Adv. Nat. Sci. Nanosci. Nanotechnol.* 9 (015008), 1–8p.
- Talebian-Kiakalaieh, Amin, Amin, Nor Aishah Saidina, Mazaheri, Hossein, 2013. A review on novel processes of biodiesel production from waste cooking oil. *Appl. Energy* 104, 683–710p.
- Venkataraman, K., 2012, May 22. Coastal and Marine Biodiversity of India. International Day for Biological Diversity Marine Biodiversity. Uttar Pradesh State Biodiversity Board.
- Wilson, Karen, Lee, Adam F., 2012. Rational design of heterogeneous catalysts for biodiesel synthesis. *Catal.Sci.Technol.* 2, 884–897p.